Monthly Notices
of the
ROYAL ASTRONOMICAL SOCIETY

Mon. Not. R. Astron. Soc. **411,** 1197–1203 (2011) doi:10.1111/j.1365-2966.2010.17760.x

Time series photometry of the nearby brown dwarf DENIS-P J0041353−562112

C. Koen★

Department of Statistics, University of the Western Cape, Private Bag X17, Bellville, 7535 Cape, South Africa

Accepted 2010 September 21. Received 2010 September 21; in original form 2009 November 21

ABSTRACT

DENIS-P J0041353−562112 is a brown dwarf, with a spectral type of M7.5, which may be younger than 20 Myr. On the basis of its Hα emission-line asymmetry, it has been suggested that the object is accreting material. If it is accreting, it is expected to rotate slowly. This paper reports on several photometric monitoring runs in the R_C and I_C bands, designed to study variability – such as that due to rotational modulation – of the object. Although there do not seem to be irregular brightness fluctuations typical of accretion, there is cyclical variability which may be due to a bright accretion-related spot. The rotation period is 2.8 h, although a double-wave variation with a period of 5.6 h cannot be ruled out completely. If the shorter period is correct, it is unlikely that the brown dwarf is disc-locked. Substantial flaring activity in the R_C band suggests a strong magnetic field.

Key words: brown dwarfs – stars: individual: DENIS-P J0041353−562112 – stars: low-mass – stars: variables: general.

1 INTRODUCTION

DENIS-P J0041353−562112 (hereinafter DENIS 0041−5621) was identified as a nearby late M dwarf by Phan-Bao et al. (2001). Phan-Bao & Bessell (2006) used spectroscopic indices to determine a spectral classification of the object, namely M7.5. In their sample of 41 late M dwarfs, it was found to have the second-strongest Hα emission. They further estimated $R - I = 2.60$ from the spectrum and $d = 17$ pc from a spectral index/absolute magnitude calibration. A closely similar spectral type of M8 was assigned by Schmidt et al. (2007). They measured the relatively large value, −4.1, of the activity indicator $\log[F(\mathrm{H}\alpha)/F(\mathrm{bol})]$. The effective temperature corresponding to the spectral type is about 2600 K (e.g. Dahn et al. 2002).

A fairly extensive study of DENIS 0041−5621 was published by Reiners (2009). A spectrum of the object showed strong Li absorption, implying that it is a relatively young brown dwarf with a mass below 0.062 $\mathrm{M}_\odot$. By comparing the spatial motion of the object with those of nearby associations, Reiners (2009) concluded that DENIS 0041−5621 may be a member of the Tuc–Hor association, at a distance of about 35 pc. The relatively large distance again implies that it is intrinsically bright and therefore young – 10 to 15 Myr. From asymmetry of the Hα line profile and the presence of Ca and He emission lines in the spectrum, it was deduced that the object is accreting, rather than magnetically active.

Accurate photometry of DENIS 0041−5621 appears in two recent sources: the DENIS catalogue (Epchtein et al. 1999; The DENIS consortium 2005) gives $I = 14.69(0.04)$, $J = 11.95(0.06)$ and $K_S = 10.88(0.07)$. The infrared magnitudes agree very well with the 2MASS values (Skrutskie et al. 2006), namely $J = 11.96(0.02)$, $H = 11.32(0.02)$ and $K_S = 10.86(0.02)$. The index $(J - K_S) \approx 1.1$ is what is expected for a late M star (Dahn et al. 2002).

Subsequent to the observations summarized above, it has been discovered that DENIS 0041−5621 has two components, separated by about 142 mas (Reiners, Seifahrt & Dreizler 2010). From near-infrared photometry, the authors estimate that the spectral types of the two components are M6.5 and M9. The contribution of the cooler component to optical flux will therefore be very small. The discovery of the binary nature of DENIS 0041−5621 has led to a substantial revision of its estimated distance: $d \sim 50$ pc, if its age is 10 Myr (71 pc, if the age is 5 Myr).

The prime observable used to diagnose accretion in DENIS 0041−5621 – asymmetry in the Hα emission line – could also have been produced by a strong magnetic flare. In principle, the rotation rate of the object could be used as a discriminant between these two alternatives. It is believed that young accreting stars/brown dwarfs rotate slowly due to so-called disc-locking (e.g. Jayawardhana et al. 2006). Slow rotation may persist for some time after cessation of accretion, but eventually the object will be spun up due to contraction. By contrast, rapid rotation is often associated with vigorous magnetic activity in late M objects (e.g. Reiners & Basri 2007). These pieces of information imply that rapid rotation would favour magnetic activity, while slow rotation would agree better with accretion as the source of the strong Hα emission.

Determining the rotation period of DENIS 0041−5621 is therefore of interest. The only way in which this can be accomplished is through monitoring the flux over time: if the surface brightness

★E-mail: ckoen@uwc.ac.za

© 2010 The Author
Monthly Notices of the Royal Astronomical Society © 2010 RAS

distribution is non-uniform, this may manifest as variability, with a period equal to the rotation period of the object. This paper reports on time series photometry of DENIS 0041−5621 obtained over the course of a week. The weather permitted observations on six nights, with run lengths from 2.6 to 8 h (Section 2). Periodic variations were seen, prompting a frequency analysis described in Section 3. The results are interpreted in Section 4.

2 OBSERVATIONS AND REDUCTIONS

Observations in the R_C and I_C bands (hereinafter referred to as R and I, respectively, for convenience) were made with the South African Astronomical Observatory (SAAO) STE4 CCD camera mounted on the SAAO 1.9-m telescope. The field of view of the camera is about 2.5 arcmin^2, which allowed one bright and three fainter comparison stars to be measured along with DENIS 0041−5621. The camera was operated in 2 × 2 pre-binning mode throughout, giving a reasonable readout time of 20 s.

A log of the observations is given in Table 1. On the first night, observations were made through the I filter; thereafter, the R filter, except for the night of 2009 October 26/27 (JD 245 5131), when observations were alternated between the two filters. Much of the observing was done through a cloud cover of variable thickness. Seeing was typically in the range 1.4–2.5 arcsec, but values worse than 3 arcsec were encountered on two nights. Given the sparseness of the field, poor seeing did not cause problems. With a pixel-scale (after pre-binning) of 0.28 arcsec pixel^{-1}, images were always well-sampled.

The choice of R and I filters was dictated by the fact that the object is very red and, for the particular telescope, relatively faint. Two filters were used in order to compare the time dependence of the flux at different wavelengths. Ideally, observations would have alternated between filters throughout, but that would have compromised the time-resolution of the measurements.

The data reductions were very simple. An automated version of the DOPHOT software (Schechter, Mateo & Saha 1993) was used to calculate profile-fitted and aperture magnitudes online. The former were considerably less noisy and therefore preferred. (This conforms to experience – default aperture sizes were used, which are not necessarily optimal for relatively faint stars. In principle, better aperture photometry could therefore be achieved, but the profile-fitted photometry is satisfactory.) The photometry was then differentially corrected. In the case of the I band, the single bright comparison star 2MASS J00412748−5623002 (hereinafter 2M 0041−5623) served as a local standard; for the R band, images of 2M 0041−5623 were generally saturated, and the two best of the three fainter stars were used as comparison stars.

Table 1. The observing log. On the fifth night only, observations were made through both the R and I filters.

Filter	Starting time (HJD 245 5100+)	Run length (h)	Exposure time (s)	N
I	26.2820	4.2	120–200	70
R	27.2524	8.0	150	141
R	28.2852	3.9	120–150	79
R	29.3043	5.9	150	63
I	31.2776	5.8	40–160	95
R	31.2696	4.1	150	60
R	32.3442	2.6	150–180	51

For both filters, the photometry was crudely placed on an absolute scale by referring to the USNO-B1.0 (Monet et al. 2003) photometry of 2M 0041−5623: $R = 12.0$ (mean of $R1$ and $R2$) and $I = 11.5$. Mean DENIS 0041−5621 magnitudes of $R \sim 16.9$, $I \sim 14.1$ are rather different from $R = 18.7$, $I = 14.7$ quoted by Phan-Bao et al. (2001), but the colour index $(R - I) \sim 2.8$ agrees well with the value 2.6 derived by Phan-Bao & Bessell (2006). Dahn et al. (2002) found $(R - I)$ indices clustering around 2.3–2.4 for late M dwarfs. A much larger sample of late-type SDSS stars was used by West, Walkowicz & Hawley (2005) to derive mean $(r - i)$ indices of 2.27 and 2.77 for M7 and M8 dwarfs, respectively. Extrapolating the transformation

$$(r - i) \approx (r' - i') = 1.00(R - I) - 0.21$$

(Rodgers et al. 2006) to redder colours, $(R - I) = 2.8$ corresponds to $(r - i) \approx 2.6$. Given that the spread in $(r - i)$ for a given magnitude is large (standard deviations of 0.20 and 0.16 for M7 and M8, respectively – West et al. 2005), $(R - I) = 2.6$–2.8 is a little red, but not inconsistent with its spectral classification of M7.5.

On the other hand, the index $(I - J) \sim 2.7$ implied by the DENIS magnitudes quoted in Section 1 is blue compared to $(i - J) \sim 3.5$–3.7 for M7–M8 stars in West et al. (2005) (standard deviations are ∼0.2 mag for both classes). This cannot easily be explained by the fact, alluded to in the Introduction section, that DENIS 0041−5621 consists of two components of unequal temperature, separated by only 0.14 arcsec on the sky. All the photometry discussed in this paper, and previously published, is for the combined components. Reiners et al. (2010) estimate that the flux from the hotter component is double that of the cool component in J: this suggests that the hotter component dominates at optical wavelengths, but that the cooler component contributes non-negligible flux in the near-infrared.

The time series of observations are plotted in Fig. 1 (R filter) and Fig. 2 (I filter). Cyclical variability, on a time-scale of about 3 h, is clearly visible. There may also be variability on a longer time-scale – see particularly the R-band observations on JD 245 5127 and both sets of I-band measurements.

Aside from these relatively slow variations, a number of rapid flares were also seen in R (Fig. 3). The first two bracketed the run on JD 245 5127, while the largest was observed during the next night. It is noteworthy that no significant flaring was seen during the other nights. It should be said though that the somewhat irregular variability in the last section of the light curve obtained on JD 245 5129 may well have been caused by low-level activity – no similar variability was seen in the other objects in the field of view.

It is unfortunately rather difficult to fully quantify the photometric accuracy of the observations. If the starfield were dense, with many stars of brightness similar to that of DENIS 0041−5621, then lightcurves could have been compared. As it is, in the case of the I filter, there is a single field star with usable photometry, which is not used in the differential standardization. It is about 1.9 mag fainter than DENIS 0041−5621; hence, the random scatter in its photometry (0.012 mag on HJD 245 5126, 0.015 mag on HJD 245 5131) is expected to be substantially larger than for the programme object. In the case of the R filter, the two field stars with the best photometry were used for standardization, leaving a single star 0.5–0.8 mag fainter than DENIS 0041−5621. The nightly standard deviations for this star varied from 0.007 mag on HJD 245 5127 to 0.018 mag on HJD 245 5132.

More qualitatively, one could consider short time-scale random scatter and longer term systematic variations. As far as the former is concerned, the reader is invited to examine the similarity between successive measurements in the light curves: this is generally

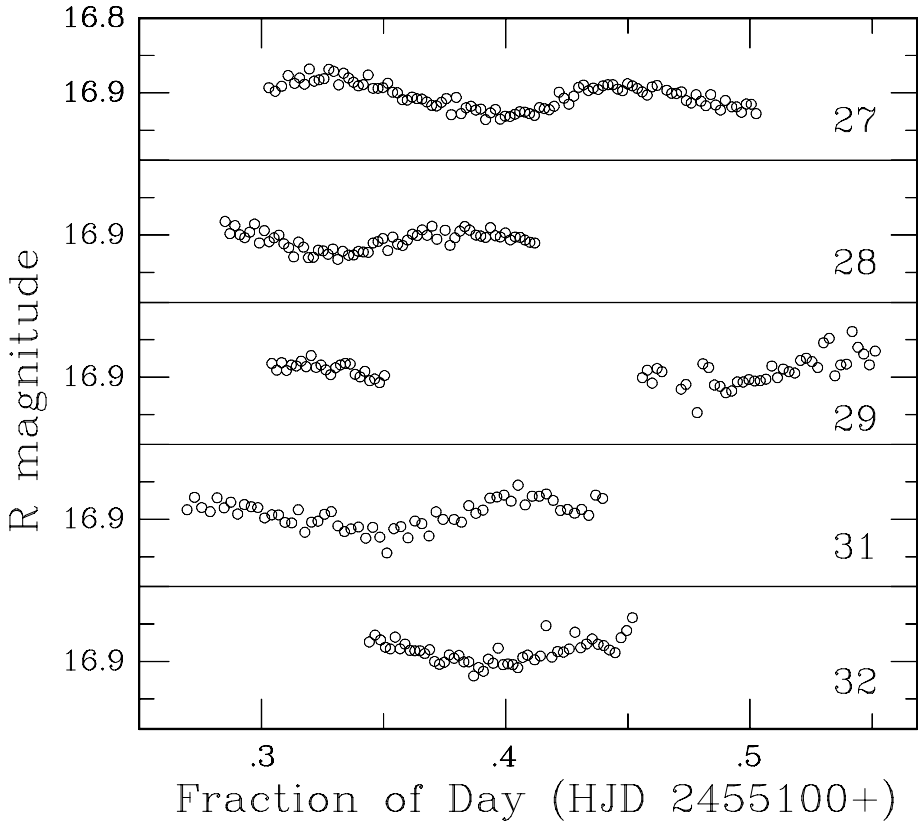

Figure 1. *R*-band observations of DENIS 0041−5621. The vertical scale on all panels is 0.19 mag. Each panel is labelled with the last two digits of the Julian Day of observation. Flares at the beginning and end of the run on HJD 245 5127 and at the end of the run on HJD 245 5128 are plotted separately in Fig. 3.

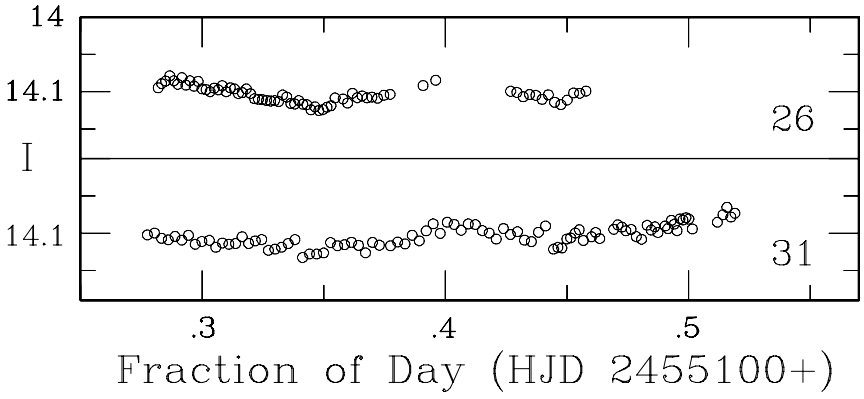

Figure 2. *I*-band observations of DENIS 0041−5621. The vertical scale on both panels is 0.19 mag. The panels are labelled with the last two digits of the Julian Day of observation.

excellent (with the exception of the last part of observations on HJD 245 5129, already remarked on above). As far as systematic variability is concerned, since the photometry has been standardized by referring it to local standards, the only potential extrinsic source of variability is in the comparison stars. However, since different local standards were selected for the two filters and different nightly comparison stars were used for the *R*-filter measurements, the cyclical variations are clearly intrinsic to DENIS 0041−5621.

3 FREQUENCY ANALYSIS

An amplitude spectrum of the *R*-band data (excluding the flares) is plotted in the top panel of Fig. 4. The aliasing pattern around the highest peak, at 8.590 d^{-1} (corresponding to a period $P = 2.794$ h), is obvious; this is due to the gaps between the strings of measurements. Although the 1 cycle d^{-1} alias at 9.59 d^{-1} cannot be rejected out of hand on the basis of the available data, inspection of the light curves in the top panel of Fig. 1, and the bottom panel of Fig. 2, shows that a period as short as $1/9.59 = 0.104$ d is unlikely. The usual convention of selecting the most-prominent alias is therefore followed; least-squares fitting of a sinusoid with $f = 8.59$ d^{-1} then gives an amplitude of 18.1 mmag.

In order to proceed, a 'pre-whitening' technique is used. In the present context, this refers to fitting a sinusoid with a particular frequency – usually that at which the spectrum reaches a global maximum – to the data and then subtracting the fit. The procedure

© 2010 The Author, MNRAS **411,** 1197–1203
Monthly Notices of the Royal Astronomical Society © 2010 RAS

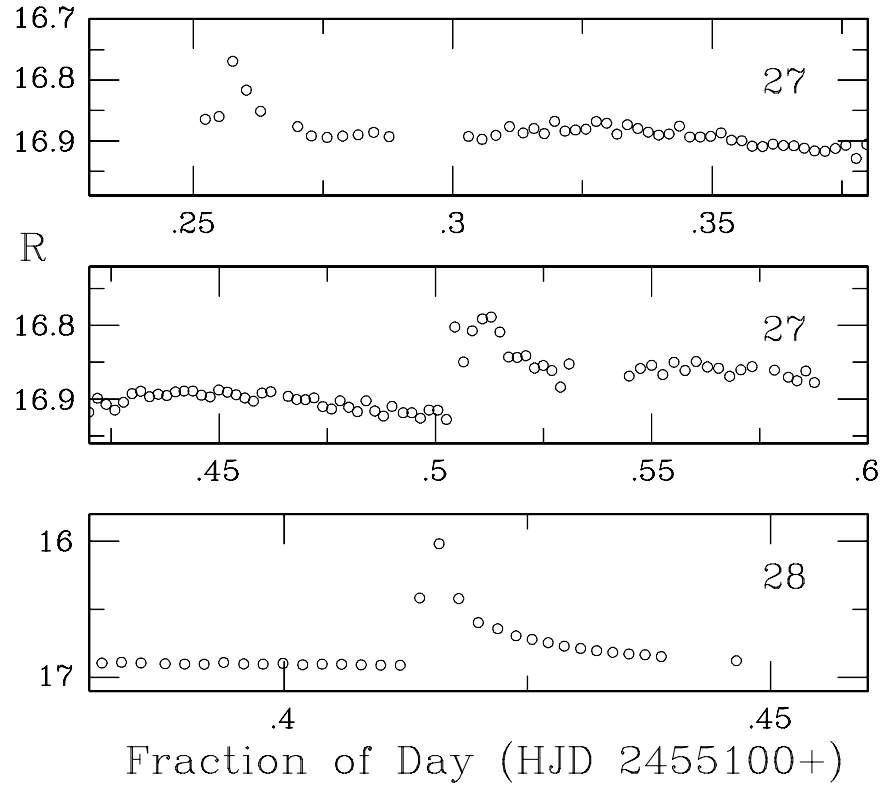

Figure 3. Substantial *R*-band flares observed during two of the runs on DENIS 0041−5621. Panels are labelled with the last two digits of the Julian Day of observation. Note that the scales of both vertical and horizontal axes differ from panel to panel. The remaining parts of the light curves for the two nights are plotted in Fig. 1.

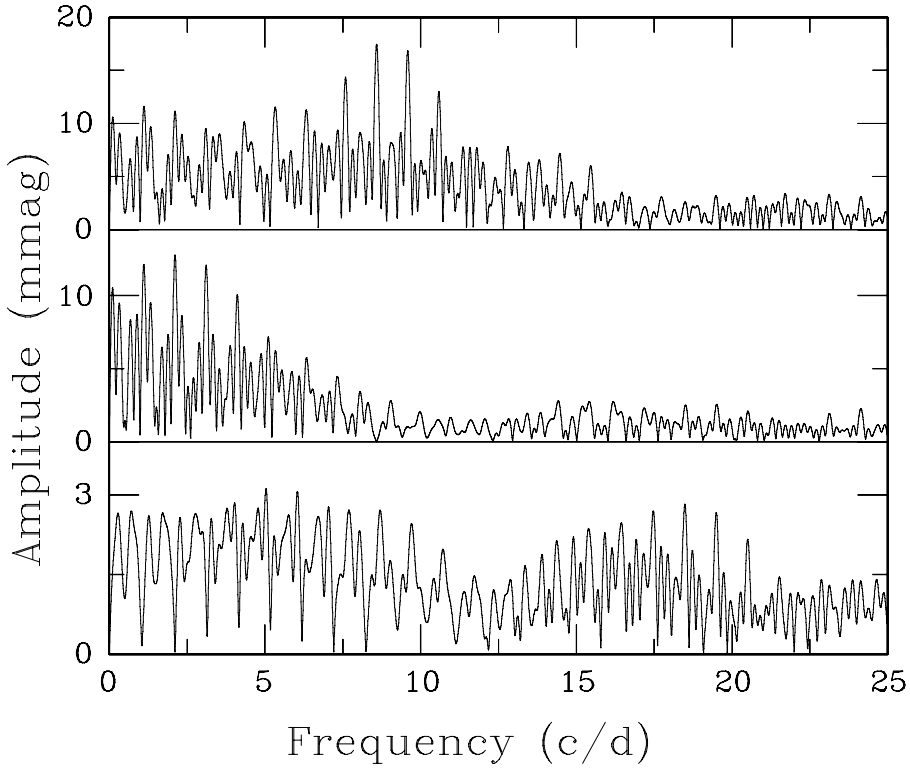

Figure 4. An amplitude spectrum of the *R*-band data (top panel). The middle and bottom panels show spectra of the residuals after pre-whitening by one and two sinusoids, respectively. Note the different scales on the vertical panels.

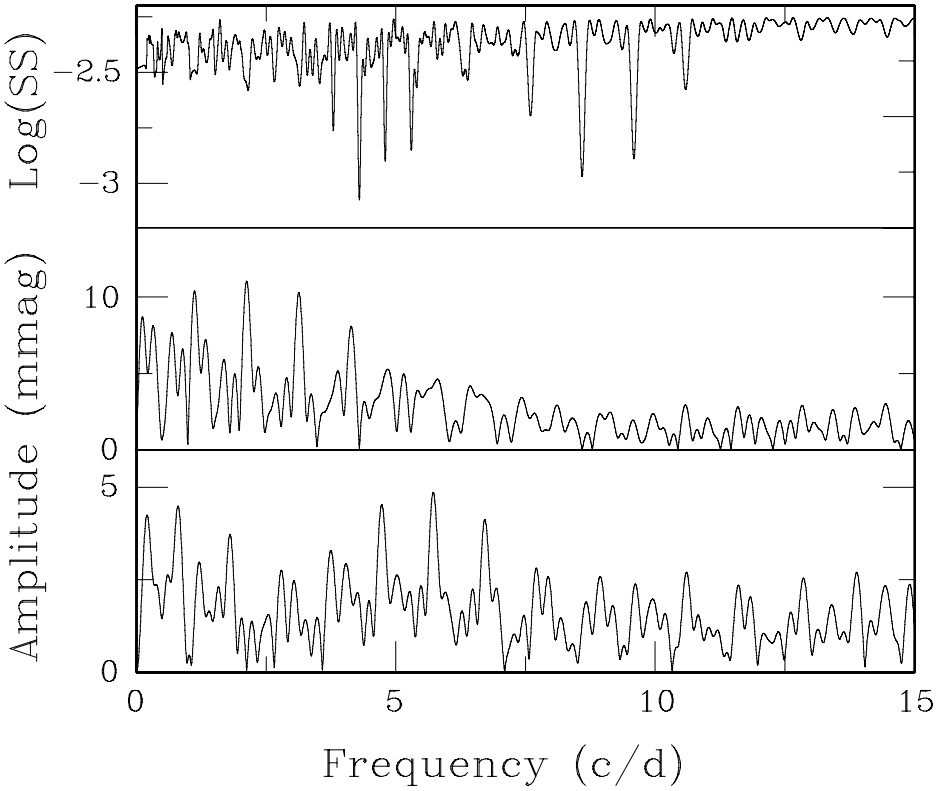

Figure 5. A residual sum-of-squares plot of a double-wave fit to the *R*-band data (top panel). The middle and bottom panels show spectra of the residuals after pre-whitening by the double wave and by the double wave plus a sinusoid, respectively. Note the different scales on the vertical panels.

'pre-whitens' the particular frequency from the observations, leaving a set of residuals for further study. The method is commonly used to extract different frequencies of multimode pulsating stars.

An amplitude spectrum of the residuals, after pre-whitening by the most-prominent feature in the top panel, can be seen in the middle panel of Fig. 4. The highest peak is at 2.114 d^{-1} (P = 11.35 h); the amplitude is 11.3 mmag. If this is also pre-whitened from the data, the residual spectrum, in the bottom panel, is obtained – it appears that the two sinusoids capture most, if not all, the signal variability in the light curves.

An alternative analysis is illustrated in Fig. 5. This is motivated by a closer look at the light curves in Fig. 1: it appears that successive cycles of the sinusoidal variation may not have the same amplitudes. This suggests the double-wave model

$$Y(t) = \mu + A_1 \cos(2\pi f t + \phi_1) + A_2 \cos(4\pi f t + \phi_2), \quad (1)$$

where μ is the mean magnitude, A_1 and A_2 are amplitudes, ϕ_1 and ϕ_2 are phases, and f is the frequency of the double wave. The values of the parameters can be estimated by minimization of the sum of squares

$$\mathrm{SS} = \sum_{j=1}^{N} \left[m(t_j) - Y(t_j)\right]^2, \quad (2)$$

where $m(t)$ is the observed magnitude and t_j is the times of the measurements. It is possible to rewrite the minimization problem in terms of the single unknown f and the top panel of Fig. 5 shows SS = SS (f). The minimum is at $f = 4.296$ d^{-1} ($P = 5.587$ h), that is, half of the leading frequency found from the amplitude spectrum in Fig. 4. The amplitudes in equation (1) are estimated as $A_1 = 7.1$ and $A_2 = 17.0$ mmag. This so-called double-wave form, in which the amplitude of the harmonic exceeds that of the fundamental frequency, is typical of light curves generated by rotation of stars with spots on opposite sides of the stars (e.g. Mantegazza et al. 1992).

The spectrum of the residuals of the double-wave fit can be seen in the middle panel of Fig. 5: the highest peak is at 2.123 d^{-1} (P = 11.30 h), very close to the most-prominent frequency in the middle panel of Fig. 4. Pre-whitening the *R*-band data by both the double wave and a sinusoid with this frequency gives residuals with the spectrum in the bottom panel of Fig. 5.

The 'Bayes Information Criterion'

$$\mathrm{BIC} = p \log N + N \log s^2 \quad (3)$$

can be used to choose between the single- and double-wave models (each with an added low-frequency component). In equation (3), N is the number of data points, s^2 is the residual variance and p is the number of model parameters. Clearly, it is desirable to minimize both the terms on the right-hand side of equation (3): the first is a measure of model complexity (the larger p, the more complex the model), while the second is a measure of how well the model fits. The 'best' model is then the one for which BIC is the smallest (see e.g. Wei 1990, or any modern text on time series analysis). According to this criterion, the two-frequency solution derived from Fig. 4 is preferred – it is simpler and the residual scatter is marginally smaller (as may have been expected from a comparison of the bottom panels of Figs 4 and 5). None the less, the fact that SS is minimized in $f = 4.296$ d^{-1} is interesting and should be pursued once a more extensive data set is available.

We proceed with the model consisting of fitting two independent frequencies to the data. More reliable parameter estimates may be obtained by fitting all parameters simultaneously, instead of relying on the sequential process described above (i.e. the successive

© 2010 The Author, MNRAS **411,** 1197–1203
Monthly Notices of the Royal Astronomical Society © 2010 RAS

Table 2. The results of fitting sinusoids to the measurements. Formal standard errors are given in brackets.

	R filter		*I* filter	
Frequency (d^{-1})	Amplitude (mmag)	Phase (rad)	Amplitude (mmag)	Phase (rad)
8.589 (0.0035)	19.6 (0.76)	2.93 (0.075)	10.4 (1.1)	−2.98 (0.11)
3.104 (0.0064)	11.5 (0.74)	2.92 (0.13)		
3.046 (0.0086)			10.1 (0.83)	−2.34 (0.082)

pre-whitening of frequencies). This is easily done by using a non-linear least-squares procedure, using the output from the sequential method to start the necessary iterations. The results are given in Table 2.

The corresponding amplitudes and phases of the *I*-band variations are also of interest, but these are much more uncertain, given the paucity of data. Two approaches were compared: fitting two sinusoids, with frequencies fixed at the values determined from the *R*-band data; and fixing the higher of the two frequencies (i.e. $8.589\,d^{-1}$) only. The residual scatter from the latter procedure was smaller and those results are therefore reported in Table 2. Note that only one of the runs had a length approaching the period (∼8 h) implied by the second frequency.

It is possible that there is a slight phase difference between the 8.589 periodicity, as seen through the two filters. The difference, modulo 2π, is 0.37 rad, with a formal standard error of 0.13 rad.

4 DISCUSSION

The ready explanation of the flares in Fig. 3 is that they are due to magnetic activity. The short-period cyclical variations in Figs 1 and 2 could, in principle, be due to either pulsation, close binarity, or spots.

It has been suggested that pulsations in young brown dwarfs could be driven by the so-called 'ϵ mechanism', that is, instability in the rate of nuclear energy generation by deuterium burning (Palla & Baraffe 2005). Interestingly, for a 0.06-$M_\odot$, brown dwarf, fundamental periods are predicted to be in the range 2.6–3.4 h. For lower mass objects, the periods are shorter – for example, Palla & Baraffe (2005) give a range of 1.0–1.7 h for $M = 0.02\,M_\odot$. However, the deuterium-processing phase is quite short lived – for example, by an age of ∼5 Myr, a 0.04-$M_\odot$, brown dwarf has depleted 99 per cent of its deuterium (Chabrier & Baraffe 2000). Given the age estimates of DENIS 0041−5621 mentioned in the Introduction section, it seems an unlikely candidate for pulsation.

The possibility that DENIS 0041−5621 is an ellipsoidal variable cannot be ruled out completely. Kepler's third law can be written as

$$\sqrt{\frac{A^3}{M_1 + M_2}} = 8.64P,$$

where A is the separation between the objects (in $R_\odot$), M_1 and M_2 are the masses of the two bodies (in $M_\odot$), and P is the period (in d). This gives a separation of

$$A = 1.593(M_1 + M_2)^{1/3},$$

assuming that the double-wave period applies. Reiners (2009) quotes a mass of 20–40 times the mass of Jupiter for DENIS 0041−5621: taking $0.02 \leq M_1 + M_2 \leq 0.08$, a separation A in the range 0.43–0.69 $R_\odot$ follows. The corresponding radial velocity semiamplitude is of the order of $(2\pi/P)(A/2) \sim 47$–$75\,km\,s^{-1}$. The fact that there are no eclipses means that any binary orbit would not be edge-on; hence, radial velocities would be reduced by a factor of $\sin i$, where i is the orbital inclination angle.

It should be noted that there have been three reported spectroscopic observations of DENIS 0041−5621 (Phan-Bao & Bessell 2006; Schmidt et al. 2007, and Reiners 2009), none of which mentions overt signs of close binarity. Given that these observations did not discover the wide binary nature of the object (Reiners et al. 2010), it is conceivable that a further cool component may also be difficult to detect directly. However, radial velocity variations may be observable, if DENIS 0041−5621 harbours a close binary.

We are therefore left with spots as the most plausible explanation for the short-period cycles. Spots may be bright, due to accretion shocks, or dark, due to magnetic effects. Unfortunately, the available information is ambiguous, as the discussion below, which draws freely on material in Stahler & Palla (2004), shows:

(i) The asymmetry of the Hα emission line, referred to in Section 1, suggests that there is accretion. Furthermore, emission lines of He I and Ca, which are often associated with accretion, are seen in the spectrum of DENIS 0041−5621 (Reiners 2009). On the other hand, the 10 per cent width of the Hα line observed by Reiners (2009) is marginal compared with those of known accretors (e.g. Jayawardhana et al. 2006). Given that the equivalent width measured by Reiners (2009) was greater than previous measurements by Phan-Bao & Bessell (2006) and Schmidt et al. (2007), the evidence for accretion is not very strong. It should also be mentioned that Hα line asymmetry, and the presence of He emission, may also be associated with magnetic flaring – see Jayawardhana et al. (2006).

(ii) Oxygen emission lines, which are good accretion indicators (e.g. Muzerolle, Hartmann & Calvet 1998), are not observed. Neither are there absorption dips on the Hα profile, indicative of winds commonly found in young pre-main-sequence objects, nor Balmer line absorption dips due to infalling material (Stahler & Palla 2004; Scholz, Jayawardhana & Brandeker 2005). This suggests that any accretion in DENIS 0041−5621 is probably at a fairly modest level.

(iii) The rapid optical flares observed on JD 245 5127 and JD 245 5128 (Fig. 3) are not known to be associated with accreting pre-main-sequence stars, but are often seen in objects with dark magnetically induced spots (e.g. Mavridis & Avgoloupis 1993; Frasca et al. 2009).

(iv) There is a non-negligible longer time-scale variation, particularly evident in the top panel of Fig. 1 and the bottom panel of Fig. 2. This is the origin of the $\sim 3\,d^{-1}$ periodicity given in Table 2. Slow variations in the transparency of circum-dwarf material is an attractive explanation for these brightness variations.

(v) With the exception of the observations obtained on JD 245 5129 (Fig. 1), there is very little evidence for irregular variability in the light curves of DENIS 0041−5621. By contrast, young, accreting objects often show continuous erratic variability (Stahler & Palla 2004, see also Koen (2008) for lightcurves of the accreting M8 brown dwarf 2M J1207334−393254).

(vi) Inspection of Table 2 shows that the amplitude of the 2.8 h periodicity is about twice as large in *R* as in *I*. Such a large increase with decreasing wavelength is typical of spots, which are hot, rather than cool. Consider the following simple model: there is a single large spot, covering a fraction $0.5f$ of the brown dwarf's surface (i.e. a fraction f of the hemisphere is covered when the spot is in the line of sight). Assume blackbody radiation at temperatures T_S

and $T_{\rm BD}$ from the spot and the unperturbed brown dwarf surface, respectively. The peak-to-peak amplitude at wavelength λ is then

$$\Delta m_\lambda = -2.5 \log \left\{ 1 - f \left[1 - \frac{B_\lambda(T_{\rm S})}{B_\lambda(T_{\rm BD})} \right] \right\},$$

where $B_\lambda(T)$ is the Planck function value at wavelength λ and temperature T (Stahler & Palla 2004). Using effective wavelengths of 6600 and 8100 Å for the R and I filters, respectively, and assuming $T_{\rm BD} = 2600$ K (see Section 1), $T_{\rm S} = 4330$ K and $f = 0.0013$ are obtained. In other words, the variability can be roughly explained by a single very small bright spot. Koen (2008) found similarly small filling factors for the accreting M8 dwarf 2MASS J1207334−393254.

(vii) It has recently been shown by Riaz & Gizis (2008) that a large fraction of brown dwarfs in the ∼10 Myr TW Hydrae association has discs, prompting the authors to suggest that discs around these objects may be longer lived than those associated with stars. If DENIS 0041−5621 is indeed somewhat older than 10 Myr, as implied by its possible membership of the Tuc–Hor association (Reiners 2009), then its age is probably close to the upper limit of disc lifetimes.

(viii) The identification of the 2.8 h period in Table 2 with the rotation period of DENIS 0041−5621 is only correct, if there is a single spot on the surface. In the case of accretion-related hotspots, it seems more likely that there will be spots associated with both the magnetic poles. Unless the brightnesses of the two spots are then precisely the same, the double-wave solution discussed in Section 3 is appropriate and the rotation period of the brown dwarf is 5.6 h. For a brown dwarf radius of $\sim 0.1\,{\rm R}_\odot$ (e.g. Chabrier & Baraffe 2000), the corresponding rotational velocities are $43\,{\rm km\,s^{-1}}$ ($P = 2.8$ h) or $22\,{\rm km\,s^{-1}}$ ($P = 5.6$ h); measurement of $v \sin i$ will possibly allow discrimination between the two alternatives and also allow determination of the inclination of the rotation axis. Mohanty, Jayawardhana & Basri (2005) have shown that most accretors are slow rotators; interestingly, the dividing line is at $v \sin i = 20\,{\rm km\,s^{-1}}$.

However, if DENIS 0041−5621 is very young, its radius may be substantially larger (e.g. table 1 of Reiners 2009), and hence $v \sin i$ may be a factor of 2 or more larger.

(ix) It is interesting to compare the results above with those of two other ultracool dwarfs for which similar time series observations are available. SSSPM J0109−5101 is of spectral type M8.5 and at a distance of about 15.5 pc (Lodieu et al. 2005). It is a field object and therefore presumably old. Koen (2005) found sinusoidal brightness modulations with a period of 7.8 h and an I-band amplitude of 19 mmag. Flares were observed in both the I and R bands, the largest in the latter filter having an amplitude of 1.6 mag. Although more energetic, the general time series attributes are, in other words, broadly similar to what is seen in DENIS 0041−5621. By contrast, 2MASS J1207334−393254 is a young (age < 10 Myr) member of the TW Hya association. It is a binary consisting of an M8 primary and an L-type secondary. The object has an apparent period of about half a day – 'apparent', because the variability is somewhat irregular, with substantially different amplitudes at different epochs (Koen 2008). Measured amplitudes were much larger than those seen in DENIS 0041−5621 and SSSPM J0109−5101, being in the range 0.1–0.2 mag in the R band.

Summarizing, there may be low-level accretion in DENIS 0041−5621, giving rise to one, or possibly two, bright shock-produced spots at or near the surface of the brown dwarf. Mid-infrared photometry could confirm the presence of a disc of cold material. Measurement of $v \sin i$ could help distinguish between the one- and two-spot models and, by implication, between magnetic and accretion activity. The object is definitely magnetically active, resembling the M8.5 field ultracool dwarf SSSPM J0109−5101.

ACKNOWLEDGMENTS

The author is grateful for telescope time made available at the SAAO and for the excellent support of the SAAO technical staff. This paper made use of material from the DENIS (Epchtein et al. 1999) and 2MASS (Skrutskie et al. 2006) catalogues. Comments from the referee helped to add flesh to the bare bones of the original version of this paper.

REFERENCES

Chabrier G., Baraffe I., 2000, ARA&A, 38, 337
Dahn C. C. et al., 2002, AJ, 124, 1170
Epchtein N. et al., 1999, A&A, 349, 236
Frasca A., Covino E., Spezzi L., Alcalá J. M., Marilli E., Fürész G., Gandolfi D., 2009, A&A, 508, 1313
Jayawardhana R., Coffey J., Scholz A., Brandeker A., van Kerkwijk M. H., 2006, ApJ, 648, 1206
Koen C., 2005, MNRAS, 357, 1151
Koen C., 2008, MNRAS, 389, 949
Lodieu N., Scholz R.-D., McCaugrean M. J., Ibata R., Irwin M., Zinnecker H., 2005, A&A, 440, 1061
Mantegazza L., Poretti E., Antonello E., Bossi M., 1992, A&A, 256, 459
Mavridis L. N., Avgoloupis S., 1993, A&A, 280, L5
Mohanty S., Jayawardhana R., Basri G., 2005, MmSAI, 76, 303
Monet D. G. et al., 2003, AJ, 125, 984
Muzerolle J., Hartmann L., Calvet N., 1998, AJ, 116, 455
Palla F., Baraffe I., 2005, A&A, 432, L57
Phan-Bao N., Bessell M., 2006, A&A, 446, 515
Phan-Bao N. et al., 2001, A&A, 380, 590
Reiners A., 2009, ApJ, 702, L119
Reiners A., Basri G., 2007, ApJ, 656, 1121
Reiners A., Seifahrt A., Dreizler S., 2010, A&A, 513, L9
Riaz B., Gizis J. E., 2008, ApJ, 681, 1584
Rodgers C. T., Canterna R., Smith J. A., Pierce M. J., Tucker D. L., 2006, AJ, 132, 989
Schechter P. L., Mateo M., Saha A., 1993, PASP, 105, 1342
Schmidt S. J., Cruz K. L., Bongiorno B. J., Liebert J., Reid I. N., 2007, AJ, 133, 2258
Scholz A., Jayawardhana R., Brandeker A., 2005, ApJ, 629, L41
Skrutskie M. F. et al., 2006, AJ, 131, 1163
Stahler S. W., Palla F., 2004, The Formation of Stars. Wiley-VCH, Weinheim
The DENIS consortium, 2005, the Third DENIS Release, available at http://cdsweb.u-strasbg.fr/denis.html
Wei W. W. S., 1990, Time Series Analysis. Addison-Wesley, Redwood City, CA
West A. A., Walkowicz L. M., Hawley S. L., 2005, PASP, 117, 706

This paper has been typeset from a TEX/LATEX file prepared by the author.